

## Adsorption of Acid Dyes on Modified Mesoporous SBA-15: Comparison of Two Dyes

M. Mirzaie<sup>a</sup>, A. Rashidi<sup>a</sup>, H.-A. Tayebi<sup>b,\*</sup> and M. Esmail Yazdanshenas<sup>c</sup>

<sup>a</sup>Department of Textile Engineering, Science and Research Branch, Islamic Azad University, Tehran, Iran

<sup>b</sup>Department of Textile Engineering, Qaemshahr Branch, Islamic Azad University, Qaemshahr, Iran

<sup>c</sup>Department of Textile Engineering, Yazd Branch, Islamic Azad University, Yazd, Iran

(Received 19 February 2018, Accepted 15 May 2018)

In this study, SBA-15-PAMAM mesoporous nano-adsorbent was synthesized, characterized and applied for adsorption of acid dyes (acid blue 62 (AB62) and acid red 266 (AR266)) from aqueous Media. Adsorption of AB62 and AR266 on SBA-15 ordered mesoporous silica, polyamidoamine functionalized SBA-15(SBA-15-PAMAM), has been investigated. To evaluate the synthesized adsorbent constructional, FT-IR (Fourier transform infrared spectroscopy), TEM transmission electron microscopy images and XRD (X-ray diffraction) methods were utilized. To investigate and compare the adsorption of two acid dyes with each other, the chemical structure and molecular mass of two acid dyes on the synthesized nano-adsorbent is compared with each other. The acid blue 62 dye with the structure of Anthrachinon ( $M_w = 422.43$ ) and the acid red 266 dye with the structure of Azo ( $M_w = 467.78$ ) is compared with each other. To appraise the proficiency of this nano-adsorbent for adsorption of two acidic dyes from aqueous media, the efficacy of significant parameters comprising pH (2-10), adsorbent dosage (0.01-0.1 g), dye concentration (200-600 mg g<sup>-1</sup>), contact time (10-120 min) and temperature (25-45 °C) was investigated. The Langmuir, Freundlich, Tempkin and Dubin Radushkevich isotherms were perused. The empirical data were best demonstrated by the langmuir isotherm model with utmost adsorption valence of (1428.57 mg g<sup>-1</sup>) for dye AB62, and (1111.11 mg g<sup>-1</sup>) for dye AR266 at pH 2 and 25 °C, in absolute agreement with the empirical data ( $R^2 > 0.9933$ ) for dye AB62 and ( $R^2 > 0.9914$ ) for dye AR266. It was concluded that SBA-15-PAMAM adsorbent could be applied as a significant adsorbent for acidic dyes removal.

**Keywords:** PAMAM dendrimer, Nano-adsorbent, SBA-15-PAMAM, Acid dyes

### INTRODUCTION

Dyes are extremely utilized in many resources, as textiles, dyeing, printing, producing of dyestuffs, paper, rubber, plastics, leather, *etc.*; and as a result, they produce a remarkable quantity of polluted wastewater [1-3].

Synthetic dyes are a significant category of rebellious organics and are mostly discovered in the environment as a result of their extensive usage. These industrial contaminants are prevalent pollutants in wastewater and are thought to decline because of their intricate aromatic structure and synthetic source. They are generated on a wide

extent [4]. Over dyeing procedure expansion and industries, one of the original contamination resources and successively a popularize problem in many countries, is dye effluent. The dye effluents could mean disastrous effects on the mammals and aquatic toxicity, and heart diseases in humans. Therefore, they should be eliminated from wastewater before offloading into water [1-5].

A category of dyes consisting sulfonic groups are acidic dyes which are generally utilized with fibers such as silk polyamide and wool. This group is distinguished from the azo group which is known as a significant and extensive category of synthetic dyes. The azo bonds could be transformed into carcinogenic and mutagenic aromatic amines over chemical reactions in water flows, causing their

\*Corresponding author. E-mail: [tayebi\\_h@yahoo.com](mailto:tayebi_h@yahoo.com)

instantaneous removal from the wastewaters [1-5]. Several chemical, physical and biological methods have been performed to remove the dyes from the wastewaters and diminish their effects on the environment. Though several biological and chemical procedures are appropriate in dye removal techniques, they need several exclusive equipment and are commonly high energy consumer. Besides, these techniques often produce excessive byproduct values. Amongst all the mentioned techniques, physical adsorptions were found to be effective and economic techniques for dye removal. Physical adsorption leads to transfer the particles from the wastewater to a solid phase by keeping the wastewater volume at an inferior range. In this case, a wide quantity of novel stuffs was utilized as adsorbents [1-3]. In the past two decades, mesoporous silica (MPS) such as SBA-15, SBA-3, MCM-48, MCM-41 were considered as potential adsorbents with a broad span of usages. These silica surfaces benefit from the identical pore formation, pore monotone structure, porous mass, thermal and mechanical consistency and ultra-wide susceptibility for modification [6-7]. Porous manufacture and texture to its excellent properties allow easier for them to provide active sites target molecule [8,9]. So, they are applied for a diversity of usages indicating their good proficiency. SBA-15, as one of the mesoporous silica compounds with high arrangement, has attracted the great interest due to its major mesoporous valence, massive surface area (3-6.5 nm), thicker pore walls, extremely thermal, hydrothermal consistency, extensive pore size (4.5-29 nm), limited distribution in other mesoporous silica constructions. Besides, it discloses the micropores attendance that is in revision to the pore frontiers. Therefore, it is essential to comprehend definition and functionalization maintenance of SBA-15 for extensive dyes adsorption valence [10]. Dendrimers are a category of molecules by an extremely branched structure with an extremely arrangement, dense structure, and some end groups which have some space among branches to absorb guest molecules. Dendrimers are safe, and have low toxicity [11]. Functionalized dendrimers prepare the probability of dye removal from liquid-solid or liquid-liquid systems [12]. In this research, SBA-15 was synthesized, functionalized by PAMAM dendrimer, and then applied as a nano adsorbent for (AB62) and (AR266) dyes removal. The efficacies of

operational parameters such as pH, SBA-15 dosage, initial dye concentration, and temperature on dye removal were investigated to evaluate the adsorption valence of SBA-15-PAMAM. The Langmuir, Freundlich, Tempkin and Dubbin Radushkevich isotherms were applied to provide appropriate equilibrium data.

## EXPERIMENTAL

### Chemicals and Methods

The TEOS (tetra-ethylorthosilicate, 99%, Merck), and the P123 surfactant (EO<sub>20</sub>PO<sub>70</sub>EO<sub>20</sub>) were prepared from Sigma-Aldrich. HCl (hydrochloric acid, 37.8%), and 3-(chloropropyl)trimethoxysilane were prepared from Merck. The C.I. acid blue 62 dye and C.I. acid red 266 were prepared by Dystar Corporation. The dyes' chemical structures are represented in Fig. 1. PAMAM dendrimer (G=0) was prepared from the (Sigma-Aldrich) (Fig. 2). Other chemicals were prepared from Merck.

For considerations the samples absorbance, the spectrometer PG instrument, and T80<sup>+</sup> UV-Vis spectrophotometer were utilized. The surface specifications of SBA-15 identified by TEM (transmission electron microscopy) perception were performed with a Hitachi, HF2000, Hitachi High-Technologies Europe GmbH and Krefeld, FTIR (Fourier transform infrared, Perkin-Elmer Spectrophotometer Spectrum 400), and also the patterns of XRD (X-ray diffraction; Bruker D8 ADVANCE with Ni-filtered Cu K $\alpha$  radiation at 1.5406 Å) were performed with a step of 0.05° and speed of 2° min<sup>-1</sup>.

### Synthesis of SBA-15

SBA-15 was synthesized based on the procedure proposed by Stucky *et.al.* [13]. Accordingly, pluronic-123 surfactant (4 g) was mixed with 125 cm<sup>3</sup> of HCL (1.9 M). The homogenized mixture was obtained by stirring consistently and continuously at a temperature of 40 °C. The TEOS (8.58 g) was then increased to the solution and stirred for 20 h. The prepared mixture was set at 100 °C for 24 h, and the obtained solution was dried, filtered and then at 550 °C was calcined for 10 h.

### Synthesis of SBA-15-Cl

SBA-15-Cl was provided by the functionalization



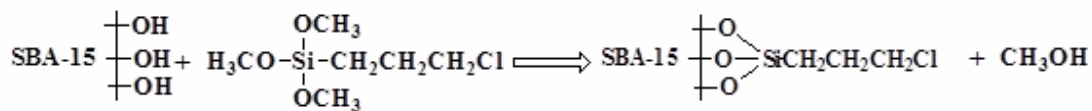


Fig. 3. Chemical structure factor of SBA-15-Cl.

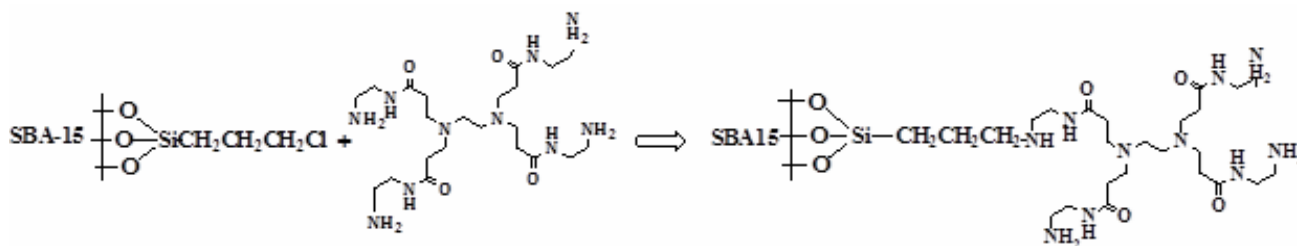


Fig. 4. Scheme of the SBA-15- PAMAM preparation.

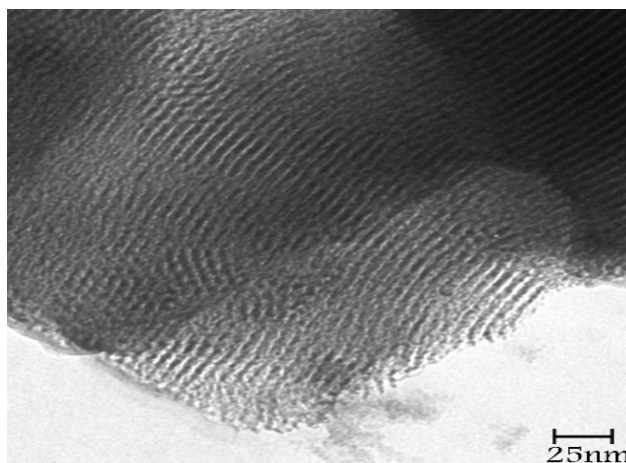


Fig. 5. TEM image of SBA-15.

the blend was refluxed at 70-80 °C for 24 h while stirring; the prepared substance was filtered, washed with toluene, ethanol and diethyl ether, and was dried at 70 °C for 8 h. The produced materials were signified as SBA-15- PAMAM (Fig. 4) [15].

The structures of SBA-15 linked with 3-chloropropyl-trimethoxysilane and PAMAM dendrimer is displayed in Figs. 3 and 4. Surface modification upon SBA-15 is applied by post-synthesis linking process. The SBA-15-Cl modification of SBA-15 was performed applying 3-chloropropyl-trimethoxysilane as the sialylation reagent. The PAMAM dendrimer's amine end groups were then

linked upon SBA-15-Cl.

### Adsorption Studies

Dye absorption mensuration was performed using (0.01-0.1 g) of SBA-15- PAMAM for AB62 and AR266 in 100 ml of (40-600 ppm) solution at different pHs (2-12) and different temperatures (25-45 °C) for various times (15-120 min). The pH of solution was adjusted by buffer solution, and at the end of the adsorption process, samples were centrifuged at a speed of 4000 rpm for 40 min to evaluate the dye concentration. The maximal wavelength of adsorption ( $\lambda_{max}$ ) was applied to define the AB62 and

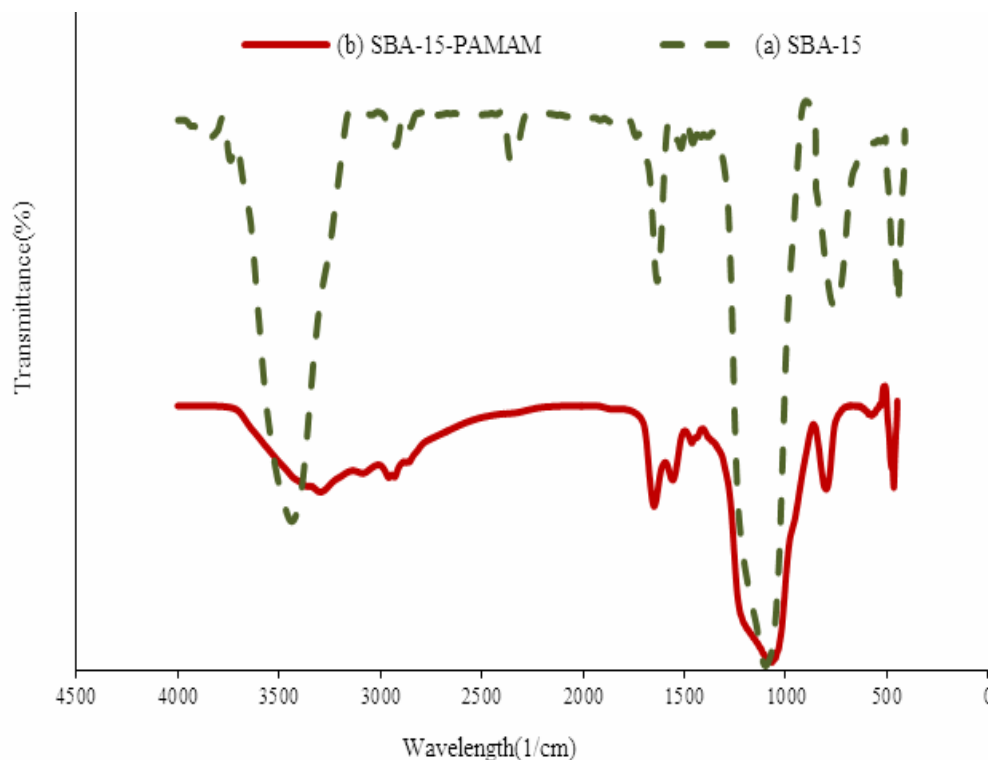


**Fig. 6.** FT-IR spectra of SBA-15 and SBA-15-Den.

AR266 concentration in the solution applying the UV-Vis spectrophotometer adjusted, respectively, at 620 nm and 524 nm.

The amount of dye adsorbed upon SBA-15- PAMAM and the percentage of dye removal were estimated by the following Eqs. (1), (2) and (3) [16,17]:

$$q_e = \frac{C_0 - C_e}{W} \times V \quad (1)$$

$$q_t = \frac{C_0 - C_t}{W} \times V \quad (2)$$

where  $q_e$  and  $q_t$  are, respectively, the amount of dye adsorbed at equilibrium and at any time upon adsorbent (SBA-15-PAMAM  $\text{mg g}^{-1}$ ).  $C_t$  is the dye concentration ( $\text{mg l}^{-1}$ ) after adsorption time  $t$ ,  $C_0$  and  $C_e$  are, respectively, the primary and ultimate concentrations of dye ( $\text{mg l}^{-1}$ ).  $W$  is the adsorbent's weight and  $V$  is the dye of bath volume.

$$R\% = \frac{A_0 - A_1}{A_0} \times 100 \quad (3)$$

Here  $R\%$  is the percentage of dye removal,  $A_1$  and  $A_0$  are, respectively, the primary dye adsorption after and before adsorption procedure.

## RESULTS AND DISCUSSIONS

### Surface Characteristics

TEM were utilized for specification of the synthesized SBA-15 morphology. Figure 5 demonstrates TEM figure via the electron beam adequate to the alignment of original SBA-15 channels. The SBA-15 demonstrates manufacturing of hexagonal full oriented mesoporous which beforehand observed by Cheng *et al.* [18,19].

Figure 6 demonstrated the SBA-15 and SBA-15-PAMAM FT-IR spectra. In SBA-15, the 801 and 1100  $\text{cm}^{-1}$  bands are dependent upon the symmetric and anti-symmetric fluctuations of Si-O-Si bond. In SBA-15, the

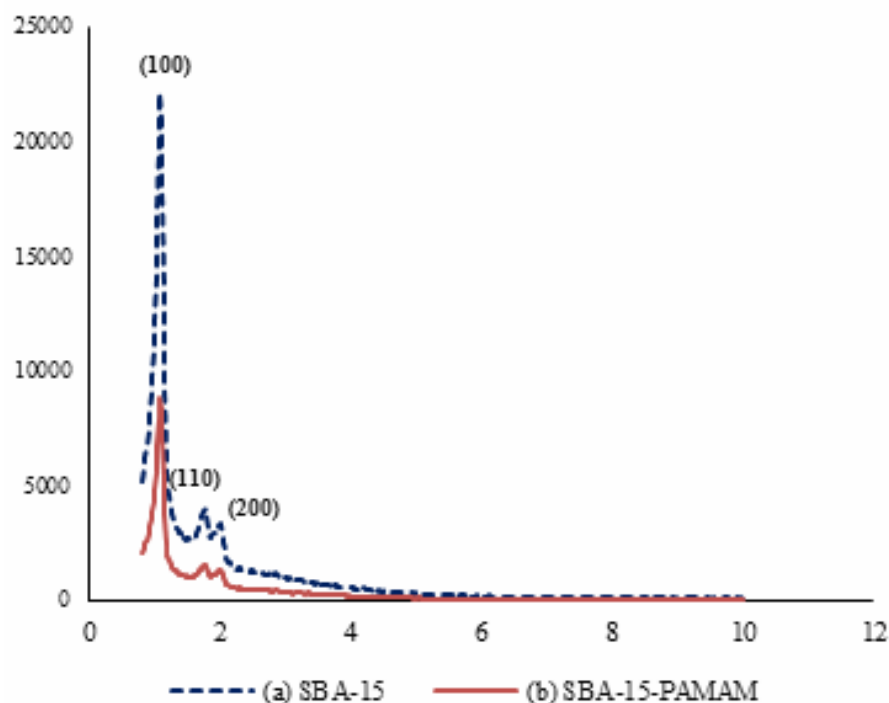


Fig. 7. Low angle XRD patterns of (a) SBA-15 and (b) SBA-Den.

band at  $3450\text{ cm}^{-1}$  with an immense absorption is attributed to the -OH fluctuations stretching of silanol groups. In SBA-15-PAMAM, the wide band at  $3411\text{ cm}^{-1}$  should be assigned to the O-H stretching arising from the fluctuations of silanol groups and water molecules adsorbed. The asymmetric and symmetric  $\text{-NH}_2$  stretching groups of SBA-15-PAMAM represent IR bands at  $3297$  and  $3411\text{ cm}^{-1}$ .

The increments in the number of SBA-15-PAMAM amine end groups indicate that the connotation of asymmetric-symmetric and the C-N stretching band and  $\text{-NH}_2$  stretching band could be comprehended at  $1462\text{-}1556\text{ cm}^{-1}$  [20-22].

Figure 7 represents the Low angle XRD patterns of SBA-15 and SBA-15-Den. The XRD patterns represents proficiently defined diffraction peak at  $2\theta = 1.1^\circ$  and two weak peaks at  $1.7^\circ$  and  $2^\circ$  due to (1 0 0), (1 1 0) and (2 0 0) reflections demonstrating the second dimensional hexagonal mesoporous structure for SBA-15. SBA-15-PAMAM was also assessed by the same pattern (Fig. 7b) representing the linking of PAMAM Dendrimer and the morphological integrity of SBA-15.

The stiffness of predominant peak at  $2\theta = 0.91$  assigned to the (100) diffraction peak [23] diminished within the

surface functionalization stages because of the diminishing the spreading strength of SBA-15 wall within functionalization [24,25].

### Adsorption Studies

**Effect of pH.** One of the substantial variables for acid dyes removal from wastewater is pH [26,27]. The adsorption valence was determined pH variations, from 2 to 12, as other variables such as the quantity of SBA-15-PAMAM nano-adsorbent, temperature and acid dye concentration are steady. The consequence of pH variations on the efficiency of dye removal is represented in Fig. 8. The dye initiative concentration and the adsorbent quantity were  $40\text{ mg l}^{-1}$  and  $0.01\text{ g}$ . The adsorption of acid dye elevates whenever pH increased from 2 to 12. According to Fig. 8, the removal efficiency at pH 2 is 77.86% and at pH 12 reduces to 4.7%. It could be conceivable the protonation of adsorbent surface at lower values of pH that expresses the poverty of acid dye molecules. Thus, probable cause of high concentration of  $\text{H}^+$  ions in extenuates pH; it should assert together with molecules of acid dye in nano-adsorbent active sites. Whereas pH increment, the rivalry among  $\text{H}^+$  ions and

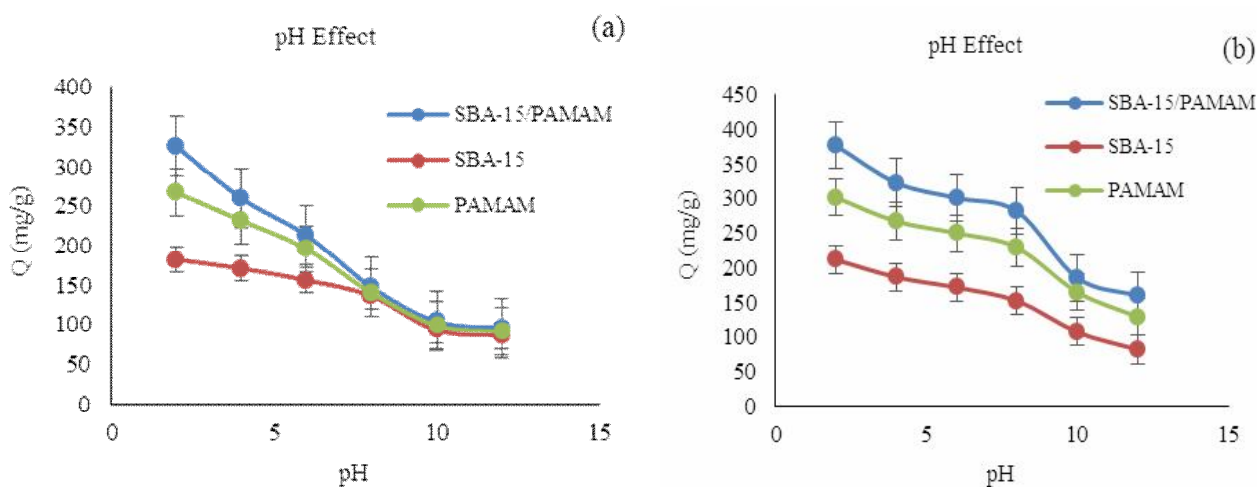


**Fig. 8.** Effect of pH on (a) AB62 and (b) AR266 removal (100 ml of  $40 \text{ mg l}^{-1}$  acid dye, time = 2 h,  $T = 25 \text{ }^\circ\text{C}$  and the amount of adsorbent = 10 mg).

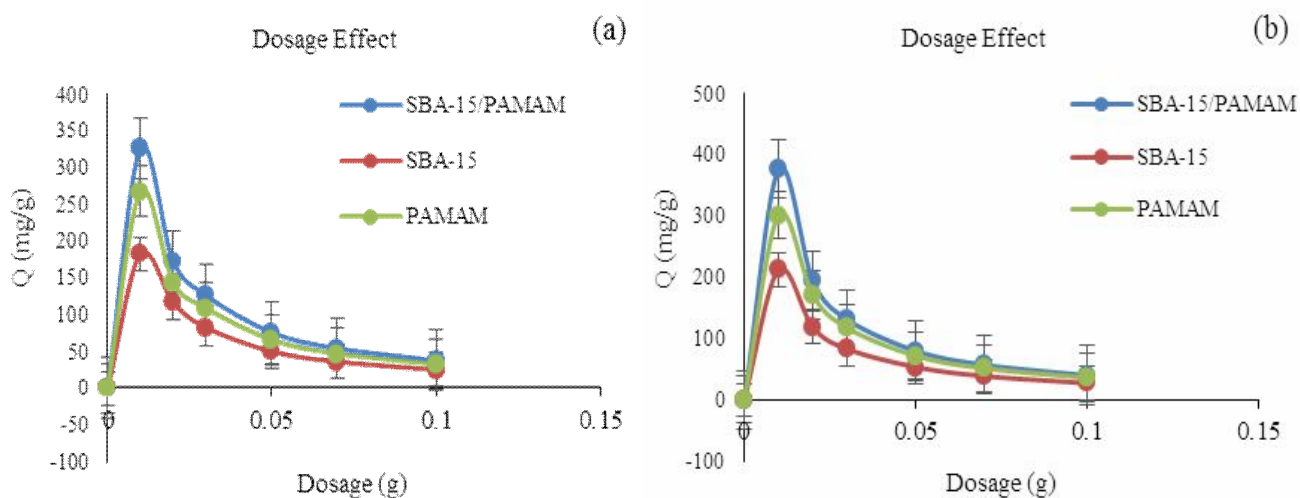


**Fig. 9.** Effect of SBA-15, SBA-15-Cl, SBA-15-PAMAM adsorbent amount on (a) AB62 and (b) AR266 removal (100 ml of acid dye solution with  $40 \text{ mg l}^{-1}$  concentration at  $25 \text{ }^\circ\text{C}$  and pH 4).

molecules of acid dye at active sites of Nano-adsorbent diminishes; terminate in diminishing adsorption valence [28].

### Effect of Adsorbent Dosage

The consequence of SBA-15-PAMAM nano-adsorbent dosage was investigated for acid dye adsorbent (0.01 to 0.1 g), at the pH of 4, and  $40 \text{ mg l}^{-1}$  dye concentration in 100 ml of acid dye solutions. The results are displayed in Fig. 9. By

elevating dosage of adsorbent up to 0.03 g, removal efficiency elevated as predicted. At quantity of 0.03 g, the maximum efficiency is 94.071%. However, addition of uttermost nano-adsorbent did not change the removal efficiency likely because of the agglomeration of nano-adsorbent molecule [29-31]. Thus, the value of Nano-adsorbent (0.03 g) is demonstrated as the optimum nano-adsorbent quantity for removal of acid dye.

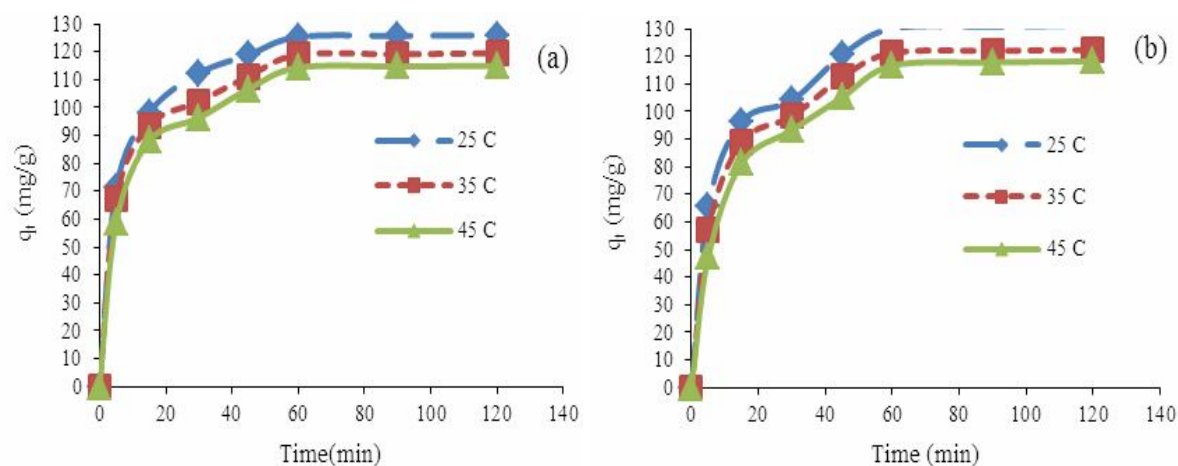


**Fig. 10.** Effect of (a) AB62, and (b) AR266 adsorption vs. contact time at various temperatures, 25, 35, 45 °C (100 ml acid dye solution with 40 mg l<sup>-1</sup> concentration, 10 mg of SBA-15-PAMAM at pH 4).

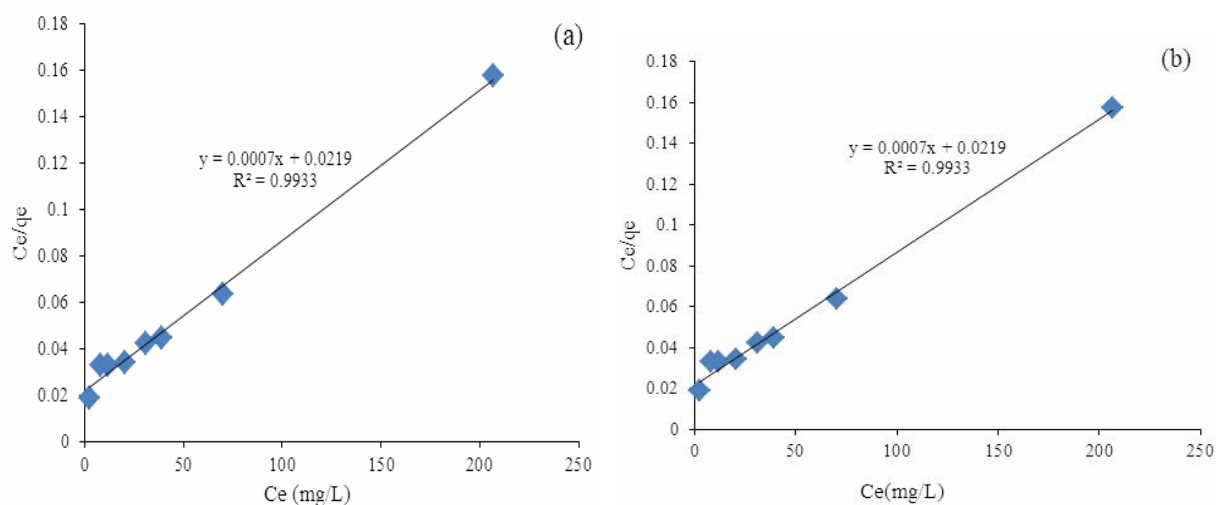


**Fig. 11.** The Langmuir isotherm plot for (a) AB62, and (b) AR266 adsorption on SBA-15-PAMAM.

### Effect of Contact Time and Temperature

Acid dyes adsorption utilizing SBA-15-PAMAM nano-adsorbent as though a subordinate of contact time was propagated as a function of time 25, 35 and 45 °C. The acquired results are displayed in Fig. 10. It could be observed that at the primary range of adsorption, dye removal has a swifter pace due to accessibility of uttermost active sites and then eventually gradual pace till the equilibrium is attained at 60 min since adsorption sites become performed [32,33].

As demonstrated in Fig. 10, the adsorbate value based on the unit adsorbent mass at time  $t$  ( $\text{mg g}^{-1}$ ),  $q_t$ , extends by elevating temperature from 25 to 45 °C demonstrating adsorption method's endothermic nature. Though, the plain, tech-economical and harmless route is carried out analysis at room temperature without any unbelievable adsorption efficiency decrement.

### Adsorption Isotherm

Adsorption is an accumulation of a mass transfer

process which could be modified as substance at the interface between two phases. Equilibrium relationships between adsorbent and adsorbate are qualified by adsorption isotherms; in general, the ratio between the adsorbed quantity and the solution residuary at a steady temperature at equilibrium. The datum of isotherm should be exactly appropriate to various isotherm models to detect an appropriate model which should be utilized for the process. Accordingly, to study the concentration efficacy that has been carried out to assign the adsorption isotherm, the analysis was accomplished at variant AB62 and AR266 concentrations, and then  $q_e$  and  $C_e$  valiancy were ascertained. Various isotherms as the Langmuir, Freundlich, Temkin and Dubbin Radushkevich isotherms were expressed. The Langmuir isotherm prosperously was utilized for disparate absorption process to demonstrate the AB62 and AR266 adsorption on SBA-15-PAMAM. The fundamental supposition is that the Langmuir theorization pending adsorbent absorption happens at adsorbent distinct sites [34-37].

The Langmuir equation would be represented as pursues:

$$q_e = \frac{Q_0 K_L C_e}{1 + K_L C_e} \quad (4)$$

as  $q_e$ ,  $c_e$ ,  $Q_0$  and  $k_L$  are AB62 and AR266 adsorbed pace over SBA-15-PAMAM ( $\text{mg g}^{-1}$ ) at the equilibrium, the AB62 and AR266 concentration solution at equilibrium ( $\text{mg l}^{-1}$ ), maximum of the adsorption valence ( $\text{mg g}^{-1}$ ), and Langmuir constant ( $\text{l g}^{-1}$ ), respectively. The Langmuir equation linear form is demonstrated by Eq. (5):

$$\frac{C_e}{q_e} = \frac{1}{K_L Q_0} + \frac{C_e}{Q_0} \quad (5)$$

The quantity of  $k_L$  and  $q_e$  amounts are computed from the slop and intercept of the  $c_e/q_e$  against  $c_e$  diagram (Fig. 11). The  $k_L$ ,  $R_f^2$  and  $q_e$  values are indexed in Table 2.

The Freundlich isotherm and its data is represented by Eq. (6) [38-40]:

$$q_e = K_F C_e^{\frac{1}{n}} \quad (6)$$

here  $1/n$  is adsorption stability and  $K_F$  is adsorption amount in concentration units.  $1/n$  valuation demonstrates that the type of isotherms is constant ( $1/n = 0$ ), undesirable ( $1/n > 1$ ), or desirable ( $0 < 1/n < 1$ ). The linear form of Eq. (7) is observed in Eq. (4):

$$\ln q_e = \ln K_F + \frac{1}{n} \ln C_0 \quad (7)$$

From the intercept and slop of  $\ln q_e$  versus  $\ln c_e$  plot, the  $K_F$  and  $n$  are calculated (Fig. 12). The Values of  $K_F$ ,  $n$  and  $R_2^2$  are mentioned in Table 2.

In Eq. (8), the Temkin isotherm is demonstrated:

$$q_e = \frac{RT}{b \ln(K_T C_e)} \quad (8)$$

In Eq. (9), the linearized form of Eq. (8) is demonstrated:

$$q_e = B_1 \ln K_T + B_1 \ln C_e \quad (9)$$

So, Eq. (10) is as bellows:

$$B_1 = \frac{RT}{b} \quad (10)$$

It is supposed that in the Temkin isotherm equation, molecules heat absorption according to adsorbate-adsorbent forces valences diminishes linearly and adsorption identified by identical distribution of the bonding energies till utmost binding energy [41-42]. The  $q_e$  versus  $\ln c_e$  plot is utilized from the intercept and slope, respectively, to define the  $K_T$  and  $B_1$  isotherm constants (Fig. 13).

The  $K_T$  ( $\text{M}^{-1}$ ) is associating of binding constant equilibrium to the uttermost binding energy, and  $B_1$  constant is the adsorption heat. Also,  $T$ ,  $b$  and  $R$ , are, respectively, definite temperature ( $K$  and  $B_1$  constant referred to adsorption heat) and the constant of universal gas ( $8.314 \text{ J mol}^{-1} \text{ k}$ ).

The isotherm model of Dubin Radushkevich (D-R) was also utilized to study the adsorption mechanism. The D-R isotherm might be utilized to modify adsorption on both heterogeneous and homogenous and surfaces [39]. The D-R isotherm linear form is:

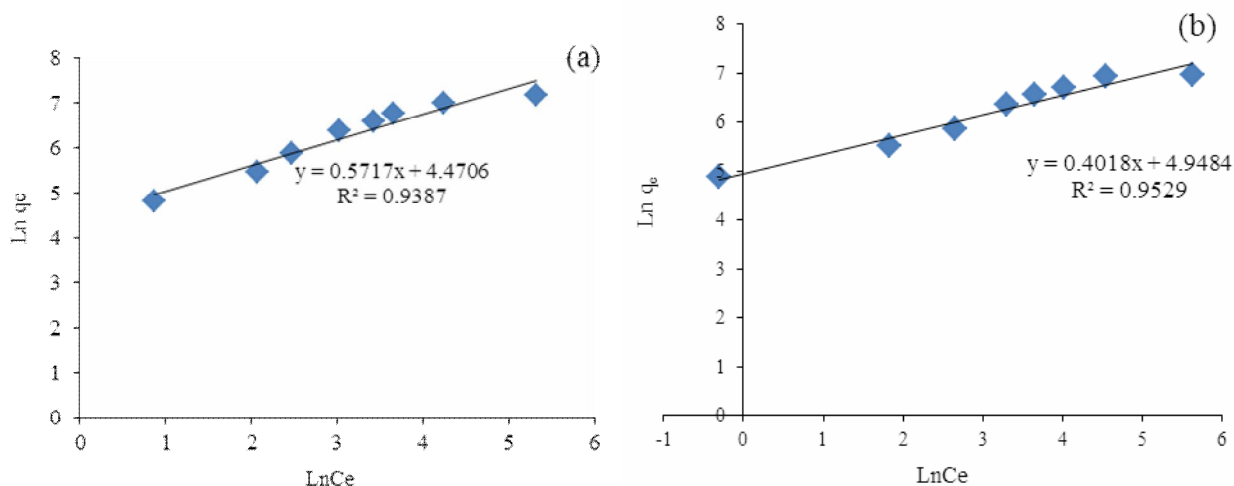


Fig. 12. The Freundlich isotherm plot for (a) AB62, and (b) AR266 adsorption on SBA-15-PAMAM.

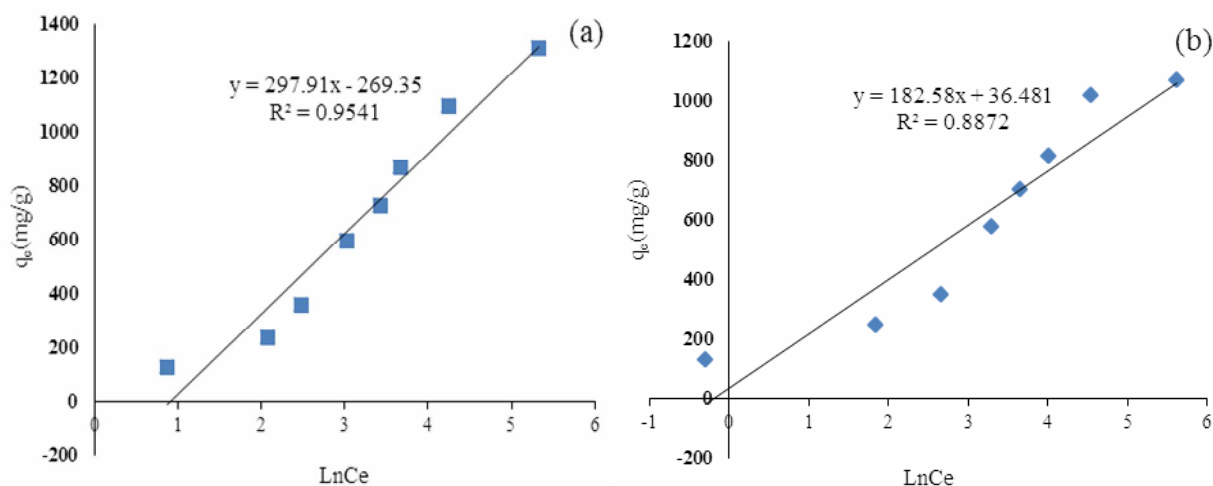


Fig. 13. The Temkin isotherm plot for (a) AB62 and (b) AR266 adsorption on SBA-15-PAMAM.

$$\ln q_e = \ln q_s - \beta \varepsilon^2 \tag{11}$$

In which  $q_m$ ,  $\varepsilon$  and  $b$  are, respectively, a constant due to the theoretical saturation valence, the Polanyi potential, and average free energy of adsorption ( $\text{mol}^2 \text{k}^{-1} \text{J}^2$ ).

The Polanyi potential is released by  $RT \ln (\ln(1 + 1/C_e))$ , where  $T$  (K) is the absolute temperature (K) and  $R$  ( $8.314 \text{ J mol}^{-1} \text{ K}$ ) is the gas constant.

In Fig. 14, the ability of the D-R isotherm to AB62 and AR266 removal by SBA-15-PAMAM was drawn by  $\ln q_e$

versus  $\varepsilon^2$ . D-R isotherm equation might be utilized to acquire  $b$  values, from where the average energy of adsorption ( $E_a$ ) could be measured by utilization of Eq. (12) [43].

$$E_a = 2\beta^{-1/4} \tag{12}$$

Due to the Eqs. (11) and (12), the correlation coefficient ( $R^2$ ) and the isotherm constants,  $E_a$  were determined. The values of  $K_L$ ,  $Q_0$ ,  $R_L$ ,  $R_1^2$  (correlation coefficients for Langmuir isotherm), and  $n$ ,  $K_F$ ,  $R_2^2$  (correlation coefficients

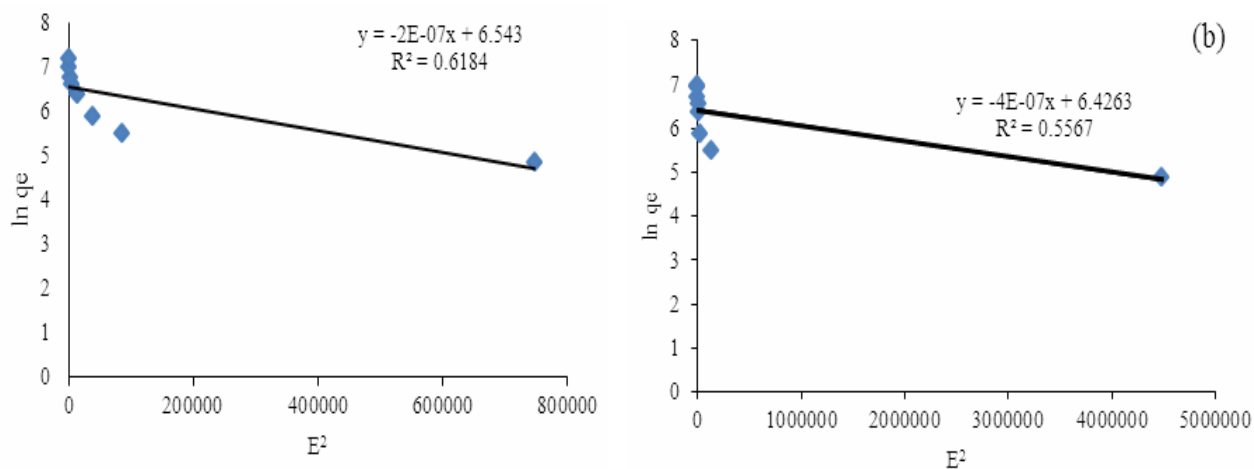


**Fig. 14.** The Dubinin radushkevich isotherm plot for (a) AB62, and (b) AR266 adsorption on SBA-15-PAMAM.

**Table 2.** Linearized Isotherm Coefficients for AB62 and AR266 Adsorbed by SBA-15-PAMAM

		Dye	
		AB62	AR266
Langmuir	$K_L$ ( $l\ g^{-1}$ )	0.032	0.048
	$Q_0$ ( $mg\ g^{-1}$ )	1428.57	1111.11
	$R_1^2$	0.9933	0.9914
	$R_L$	0.0725	0.339
Freundlich	$K_F$ ( $(mg\ g^{-1}) (l\ mg^{-1/n})$ )	87.41	140.95
	$n$	1.7492	2.489
	$R_2^2$	0.9387	0.9529
Temkin	$K_T$ ( $l\ g^{-1}$ )	0.4049	1.221
	$B_1$ ( $kJ\ mol^{-1}$ )	297.91	182.58
	$R_3^2$	0.9541	0.8872
Dubin	$K_{D-R}$ ( $mol^2\ k^{-1/2}$ )	0.2	0.4
Radushkevich	$q_m$ ( $mg\ g^{-1}$ )	694.37	617.88
	$R_4^2$	0.6184	0.5567
	$E_a$ ( $kJ\ mol^{-1}$ )	1.581	1.118

**Table 3.** Comparison of Anionic Dyes Adsorption onto Various Adsorbents

Adsorbent	Dye	q <sub>m</sub> (mg/g)	Ref.
Magnetic ZnFe <sub>2</sub> O <sub>4</sub>	Acid red 88	111.1	[46]
SBA-3/PEHA	Acid yellow 127	1250	[47]
MCM-41/NH <sub>3</sub> <sup>+</sup>	Acid violet 19	251.76	[48]
Chitosan	Acid red 18	693.2	[49]
Activated carbon	Acid red 97	52.08	[50]
Activated red mud	Acid blue 113	83.33	[51]
MCM-41/PPy	Acid blue 129	63.36	[52]
MCM-41/APTMS	Acid blue 62	55.55	[53]
MCM-41/APTMS	Acid blue 25	45.9	[54]
MCM-4/PPy	Direct blue 6	11.8	[55]
MRH-HCl/PAni	Acid blue 62	55.55	[56]
AC-NP-Ag	Acid red 18	100	[57]
AC-NW-Cd(OH) <sub>2</sub>	Orange yellow S	37	[58]
SBA-15-PAMAM	Orange yellow S	76.9	[58]
SBA-15-PAMAM	Acid blue 62	1428.57	This study
SBA-15-PAMAM	Acid red 266	1111.11	This study

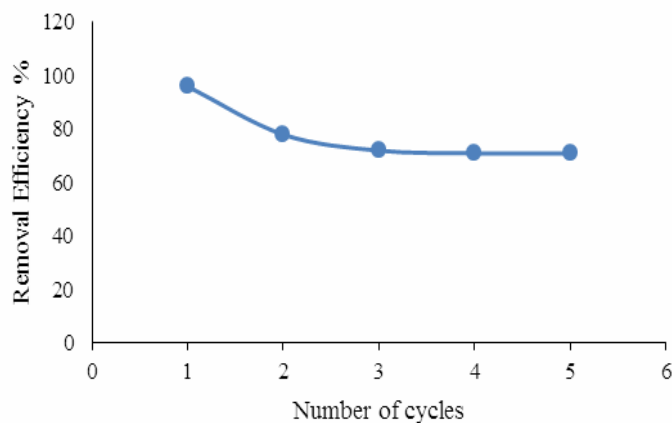


**Fig. 15.** Regeneration studies of SBA-15-PAMAM. (pH (2), adsorbent dosage (0.3 g l<sup>-1</sup>), contact time (120 min)).

for Freundlich isotherm), and  $B_1$ ,  $K_T$  and,  $R_3^2$  (correlation coefficients for Temkin isotherm) and the amounts of  $\beta$ ,  $q_m$ , and  $R_4^2$  (the correlation coefficients for Dubinin radushkevich isotherm) are represented in Table 2.

The coordinate of a model to the experimental data are generally assessed in title of linear regression analysis that the R2 value is utilized as a sign for the excellence of model fit concerning to R2 amounts (Table 2), the adsorption of AB62 and AR266 on the SBA-15-PAMAM might be assessed as a procedure that mainly pursues the Langmuir model.

The Langmuir model data demonstrated in Table 2 proposed that AB62 and AR266 adsorptions ( $R^2 = 0.9933$  and  $R^2 = 0.9914$ ) have created a monolayer coverage on the surface of adsorbent through which all adsorption sites behave equally with uniform adsorption energies without any interaction amongst the adsorbed molecules [34-35].

The uttermost SBA-15-PAMAM adsorption valence might be described to proceed through electrostatic interactions and hydrogen bond formation amongst the adsorbent surface and acid dyes. In the aqueous media, the dyes sulfonate group separate and are transformed to anionic ions. Further, in the presence of  $H^+$ , the SBA-15-PAMAM amine groups are protonated. Subsequently the electrostatic attraction might take place amongst the acid dyes negatively charged sulfonate groups ( $-SO_3^-$ ) and the positively charged protonated amino groups on the silica surface ( $-NH_3^+$ ). In addition, the major diagnosis of the acid dyes is the amount of hydrophilic functional groups, which have an intense inclination to form hydrogen bonds with SBA-15-PAMAM [44].

The observed nature of the adsorption isotherms for all of the routes showed that there is a tendency for large adsorbed molecules to affiliate with their surfaces than to stay as separated units through adsorption. Besides, the results propose that molecularly impressed materials might be planed for vast adsorption valence without flexibility the selectivity [44-45].

The acid dyes removal results represented in the literature by various sorbents are displayed in Table 3. As demonstrated in this table, the utmost adsorption valences of SBA-15-PAMAM obtained for AB62 and AR266 in this research are analogous, 1428.57 and 1111.11  $mg\ g^{-1}$ , which

are more than other sorbents in the literature. The greater adsorption valence of the adsorbent utilized in this research might be obtained from SBA-15-PAMAM characteristics.

### Adsorption and Desorption Studies

By accomplishing desorption appraisements, we could assess the mechanism of adsorption and adsorbent reuse ability. The interaction of dye molecules with the adsorbent surface (either a weak or a strong bond) ascertains the adsorption reversibility. The desorption considerations were performed utilizing NaOH solution (pH 10) to desorb AB62 dye from SBA-15-PAMAM. The desorption considerations for five cycles are represented in Fig. 15. Results represented 15% subsidence in the adsorption valence after first regeneration cycle (Fig. 15). This reduction in adsorption valence could be due to the damage or decomposition established by the alkaline solution to specify functional groups present on the SBA-15-PAMAM surface. The decrease in the adsorption valence for the second and third cycles was about 7%. The removal valence residue was nearly constant (75%) for the successive cycles (up to three cycles) representing that the adsorbent could be utilized for many times without any excessive decrease in adsorption valence [59].

## CONCLUSIONS

Regarding to this study, SBA-15-PAMAM mesoporous nano-adsorbent was synthesized. The TEM image represents the SBA-15 mesoporous cylindrical pore formation and a well-organized hexagonal arrangement and also an extensive specific area. Also, the results of the TEM images, FTIR, XRD represent the successful functionalization of PAMAM on the SBA-15 pore wall. The SBA-15-PAMAM nano-adsorbent is an appropriate adsorbent for AB62 and AR266 dyes removal. The utmost elimination was represented by 0.3  $g\ l^{-1}$  nano-adsorbent at  $pH = 2$  at 60 min contact time, and 25 °C. The obtained datum was in an excellent agreement with the Langmuir isotherm. The SBA-15-PAMAM nano-adsorbent adsorption ability (1428.57 and 1111.11  $mg\ g^{-1}$  for AB62 and AR266, respectively) was obtained by Langmuir isotherm. At a certain concentration of two acidic dyes (acid blue 62 and acid red 266), since the molecular mass of the acid blue 62

dye is less than acid red 266 and the available number of functional groups of dye molecules supposed to adsorb on the adsorbent, in acid blue 62 dye are more than those for acid red 266, the maximum amount of absorption ( $q_{\max}$ ) of acid blue 62 dye will be higher than that for acid red 266 leading to a higher uptake capacity over the surface.

## REFERENCES

- [1] Javadian, H. R.; Ghorbani, F.; Tayebi, H. A.; Hosseini Asl, S. M., Study of the adsorption of Cd(II) from aqueous solution using zeolite-based geopolymer, synthesized from coal fly ash; kinetic, isotherm and thermodynamic studies, *Arab. J. Chem.* **2015**, *8*, 837-849, DOI: org/10.1016/j.arabjc.2013.02.018.
- [2] Gan, Y.; Tian, Na.; Tian, X.; Ma, L.; Wang, W.; Yang, C.; Zhou, Z.; Wang, Y., Adsorption behavior of methylene blue on amine-functionalized ordered mesoporous alumina. *J. Porous Mater.* **2015**, *22*, 147-155, DOI: 10.1007/s10934-014-9881-9.
- [3] Anbia, M.; Salehi, S., Removal of acid dyes from aqueous media by adsorption onto amino-functionalized nanoporous silica SBA-3. *Dyes Pigm.* **2012**, *94*, 1-9, DOI: 10.1016/j.dyepig.2011.10.016.
- [4] Crini, G.; Badot, P. M., Application of chitosan, a natural aminopolysaccharide, for dye removal from aqueous solutions by adsorption processes using batch studies: a review of recent literature, *Prog. Polym. Sci.* **2008**, *33*, 399-447, DOI: org/10.1016/j.progpolymsci.2007.11.001.
- [5] Qin, Q.; Ma, J.; Liu, K., Adsorption of anionic dyes on ammonium-functionalized MCM-41. *J. Hazard. Mater.* **2009**, *162*, 133-139, DOI: 10.1016/j.jhazmat.2008.05.016.
- [6] Yan, Z.; Li, G.; Mu, L.; Tao, S., Pyridine-functionalized mesoporous silica as an efficient adsorbent for the removal of acid dyestuffs. *J. Mater. Chem.* **2006**, *16*, 1717-1725, DOI: 10.1039/B517017F.
- [7] Chen, Z.; Zhou, L.; Zhang, F.; Yu, C.; Wei, Z., Multicarboxylic hyperbranched polyglycerol modified SBA-15 for the adsorption of cationic dyes and copper ions from aqueous media. *Appl. Surf. Sci.* **2012**, *258*, 5291-5298, DOI: org/10.1016/j.apsusc.2012.02.021.
- [8] Huang, C. H.; Chang, K. P.; Ou, H. D.; Chiang, Y. C.; Wang, C. F., Adsorption of cationic dyes onto mesoporous silica, *Micropor. Mesopor. Mater.* **2011**, *141*, 102-109, DOI: org/10.1016/j.micromeso.2010.11.002.
- [9] Shafiabadi, M.; Dashti, A.; Tayebi, H. A., Removal of Hg(II) from aqueous solution using polypyrrole/SBA-15 nanocomposite: Experimental and modeling. *Synth. Met.* **2016**, *212*, 154-160, DOI: org/10.1016/j.synthmet.2015.12.020.
- [10] Zhao, A.; Samanta, A.; Sarkar, P.; Gupta, R., Carbon dioxide adsorption on amine-impregnated mesoporous SBA-15 sorbents: Experimental and kinetics study. *Ind. Eng. Chem. Res.* **2013**, *52*, 6480-6491, DOI: 10.1016/j.watres.2006.07.008.
- [11] Choi, Y. S.; Cho, T. S.; Kim, J. M.; Han, S. W.; Kim, S. K., Amine terminated G-6 PAMAM dendrimer and its interaction with DNA probed by Hoechst 33258, *Biophys. Chem.* **2006**, *121*, 142-149, DOI: org/10.1016/j.bpc.2006.01.005.
- [12] Burkinshaw, S. M.; Froehling, P. E.; Mignanelli, M., the effect of hyperbranched polymers on the dyeing of polypropylene fibres, *Dyes Pigm.* **2002**, *53*, 229-235, DOI: org/10.1016/S0143-7208(02)00006-2.
- [13] Boettcher, S. W.; Fan, J.; Tsung, C. K.; Shi, Q.; Stucky, G. D., Harnessing the sol-gel process for the assembly of non-silicate mesostructured oxide materials, *Acc. Chem. Res.* **2007**, *40*, 784-792, DOI: 10.1021/ar6000389.
- [14] Adam, F.; Osman, H.; Hello, K. M., The immobilization of 3-(chloropropyl) triethoxy silane onto silica by a simple one-pot synthesis, *J. Colloid Interface Sci.* **2009**, *331*, 143-147, DOI: org/10.1016/j.jcis.2008.11.048.
- [15] Bhagiyalakshmi, M.; Yun, L. J.; Anuradha, R.; Jang, H. T., Utilization of rice husk ash as silica source for the synthesis of mesoporous silicas and their application to CO<sub>2</sub> adsorption through TREN/TEPA grafting, *J. Hazard. Mater.* **2010**, *175*, 928-938, DOI: org/10.1016/j.jhazmat.2009.10.097.
- [16] Tayebi, H. A.; Yazdanshenas, M. E.; Rashidi, A.; Khajavi, R.; Montazer, M., The Isotherms, kinetics, and Thermodynamics of Acid Dye on Nylon 6 with different amounts of titania and fiber cross sectional

- shape. *J. Eng. Fiber Fabr.* **2015**, *10*, 97-108.
- [17] Akbartabar, I.; Yazdanshenas, M. E.; Tayebi, H. A.; Nasirizadeh, N., Physical chemistry studies of acid dye removal from aqueous media by mesoporous nano composite: Adsorption isotherm, kinetic and thermodynamic studies. *Phys. Chem. Res.* **2017**, *5*, 659-679, DOI: 10.22036/pcr.2017.83378.1371.
- [18] Cheng, Q.; Pavlinek, V.; Li, C.; Lengalova, A.; He, Y.; Saha, P., Synthesis and characterization of new mesoporous material with conducting polypyrrole confined in mesoporous silica, *Mater. Chem. Phys. J.* **2006**, *98*, 504-508, DOI: org/10.1016/j.matchemphys.2005.09.074.
- [19] Aghajani, Kh.; Tayebi, H. A., Synthesis of SBA-15/PAni mesoporous composite for adsorption of reactive dye from aqueous media: RBF and MLP networks predicting models. *Fiber. Polym.* **2017**, *18*, 465-475, DOI: 10.1007/s12221-017-6610-4.
- [20] Adam, F.; Balakhrisnan, S.; Wong, P. L., Rice husk ash silica as a support material for ruthenium based heterogenous catalyst, *J. Phys. Sci.* **2006**, *17*, 1-13.
- [21] Brodoloi, A.; Mathew, N. T.; Lefebvre, F.; Haligudi, S. B., Inorganic-organic hybrid materials based on functionalized silica and carbon: A comprehensive understanding toward the structural property and catalytic activity difference over mesoporous silica and carbon supports, *Microporous Mesoporous Mater.* **2008**, *115*, 345-355, DOI: org/10.1016/j.micromeso.2008.02.005.
- [22] Sadeghi-Kiakhani, M.; Tayebi, H. A., Eco-friendly reactive dyeing of modified silk fabrics using corona discharge and chitosan pre-treatment. *J. Text. Inst.* **2017**, *108*, 1164-1172, DOI: org/10.1080/00405000.2016.1222861.
- [23] Ullah, R.; Atilhan, M.; Aparicio, S.; Canlier, A.; Yavuz, C. T., Insights of CO<sub>2</sub> adsorption performance of amine impregnated mesoporous silica (SBA-15) at wide range pressure and temperature conditions. *Int. J. Greenh. Gas Control.* **2015**, *43*, 22-32, DOI: 10.1016/j.ijggc.2015.09.013.
- [24] Bui, T.; Choi, H., Adsorptive removal of selected pharmaceuticals by mesoporous silica SBA-15. *J. Hazard. Mater.* **2009**, *168*, 602-608, DOI: 10.1016/j.jhazmat.2009.02.072.
- [25] Golshan Tafti, A.; Rashidi, A.; Tayebi, H. A., Yazdanshenas, M. E., Comparison of different kinetic models for adsorption of acid blue 62 as an environmental pollutant from aqueous solution onto mesoporous Silicate SBA-15 modified by tannic acid. *Int. J. Nano Dimen.* **2018**, *9*, 79-88.
- [26] Ballav, N.; Maity, A.; Mishra, Sh. B., High efficient removal of chromium(VI) using glycine doped polypyrrole adsorbent from aqueous solution, *Chem. Eng. J.* **2012**, *198*, 536-546, DOI: org/10.1016/j.apsusc.2010.12.146.
- [27] Ghaharpour, M.; Abousaeed Rashidi, A.; Tayebi, H., Adsorption behavior of disperse orange 30 on polyester fabric. *World Appl. Sci. J.* **2011**, *14*, 1291-1295.
- [28] Shahbazi, A.; Younesi, H.; Badiiei, A.; Functionalized SBA-15 mesoporous silica by melamine-based dendrimer amines for adsorptive characteristics of Pb(II), Cu(II) and Cd(II) heavy metal ions in batch and fixed bed column, *Chem. Eng. J.* **2011**, *168*, 505-518, DOI: org/10.1016/j.cej.2010.11.053.
- [29] Arshadi, M., Manganese chloride nanoparticles: a practical adsorbent for the sequestration of Hg(II) ions from aqueous solution, *Chem. Eng. J.* **2015**, *259*, 170-182, DOI: org/10.1016/j.cej.2014.07.111.
- [30] Kakavandi, B.; Kalantary, R. R.; Farzadkia, M.; Mahvi, A. H.; Esrafilii, A.; Azari, A.; Yari, A. R.; Javid, A. B., Enhanced chromium(VI) removal using activated carbon modified by zero valent iron and silver bimetallic nanoparticles. *J. Environ. Health Sci. Eng.* **2014**, *12*, 115, DOI: org/10.1186/s40201-014-0115-5.
- [31] Zareyee, D.; Tayebi, H.; Javadi, S. H., Preparation of polyaniline/activated carbon composite for removal of reactive red 198 from aqueous solution. *Iran. J. Org. Chem.* **2012**, *4*, 799-802.
- [32] Zhong, Q. Q.; Yue, Q. Y.; Li, Q.; Xu, X.; Gao, B. Y., Preparation, characterization of modified wheat residue and its utilization for the anionic dye removal, *Desalin. Water Treat.* **2011**, *267*, 193-200, DOI: org/10.1016/j.desal.2010.09.025.
- [33] Tayebi, H.; Dalirandeh, Z.; Shokuhi Rad, A.; Mirabi, A.; Binaeian, E., Synthesis of polyaniline/Fe<sub>3</sub>O<sub>4</sub> magnetic nanoparticles for removal of reactive red 198 from textile waste water: kinetic, isotherm and

- thermodynamic studies. *Desal. Water Treat.* **2016**, *57*, 22551-22563, DOI: 10.1080/19443994.2015.1133323.
- [34] Liu, L.; Zhang, B.; Zhang, Y.; He, Y.; Huang, L.; Tan, S.; Cai, X., Simultaneous removal of cationic and anionic dyes from environmental water using montmorillonite-pillared graphene oxide. *J. Chem. Eng. Data.* **2015**, *60*, 1270-1278, DOI: 10.1021/je5009312.
- [35] Alqadami, A. A.; Naushad, M.; Abdalla, M. A.; Ahamad, T.; Abdullah Alothman Z.; Alshehri, S. M., Synthesis and characterization of Fe<sub>3</sub>O<sub>4</sub>@TSC nanocomposite: highly efficient removal of toxic metal ions from aqueous medium. *RSC Adv.* **2016**, *6*, 22679-22689, DOI: 10.1039/C5RA27525C.
- [36] Crini, G.; Badot, P. M., Application of chitosan, a natural amino poly saccharide, for dye removal from aqueous solutions by adsorption processes using batch studies: A review of recent literature, *Prog. Polym. Sci.* **2008**, *33*, 399-447, DOI: org/10.1016/j.progpolymsci.2007.11.001.
- [37] Tayebi, H., Synthesis of polyaniline/nanosilica nanocomposite for removal of reactive orange 16 from aqueous solutions. *Iran. J. Org. Chem.* **2016**, *8*, 1737-1744.
- [38] Alley, E. R., Water Quality Control Handbook. London. McGraw-Hill Professional, 2000.
- [39] Lu, M.; Lü, X.; Xu, X.; Guan, X., Thermodynamics and kinetics of bacterial cellulose adsorbing persistent pollutant from aqueous solutions. *Chem. Res. Chin. Univ.* **2015**, *31*, 298-302, DOI: 10.1007/s40242-015-4275-3.
- [40] Lu, X.; Shao, Y.; Gao, N.; Ding, L., Equilibrium, thermodynamic, and kinetic studies of the adsorption of 2,4-dichlorophenoxyacetic acid from aqueous solution by MIEX resin. *J. Chem. Eng. Data.* **2015**, *60*, 1259-1269, DOI: 10.1021/je500902p.
- [41] Zhang, G.; Yi, L.; Deng, H.; Sun, P., Dyes adsorption using a synthetic carboxymethyl cellulose-acrylic acid adsorbent. *J. Environ. Sci.* **2014**, *26*, 1203-1211, DOI: org/10.1016/S1001-0742(13)60513-6.
- [42] Wang, Y.; Zhao, L.; Peng, H.; Wu, J.; Liu, Z.; Guo, X., Removal of anionic dyes from aqueous solutions by cellulose-based adsorbents: Equilibrium, kinetics, and thermodynamics. *J. Chem. Eng. Data.* **2016**, *61*, 3266-3276, DOI: 10.1021/acs.jced.6b00340.
- [43] Aghajani, K.; Tayebi, H. A., Adaptive neuro-fuzzy inference system analysis on adsorption studies of reactive red 198 from aqueous solution by SBA-15/CTAB composite. *Spectrochim. Acta, Part A* **2017**, *171*, 439-448, DOI: 10.1016/j.saa.2016.08.025.
- [44] Anbia, M.; Salehi, S., Removal of acid dyes from aqueous media by adsorption onto amino-functionalized nanoporous silica SBA-3, *Dyes Pigm.* **2012**, *94*, 1-9, DOI: org/10.1016/j.dyepig.2011.10.016.
- [45] Escobar, C. C. D.; Santos, F. J. H. Z. D., Effect of a sol-gel route on the preparation of silica-based sorbent materials synthesized by molecular imprinting for the adsorption of dyes. *Ind. Eng. Chem. Res.* **2015**, *54*, 254-262, DOI: 10.1021/ie503993d.
- [46] Konicki, W.; Sibera, D.; Mijowska, E.; Lendzion-Bielun, Z.; Narkiewicz, U., Equilibrium and kinetic studies on acid dye acid red 88 adsorption by magnetic ZnFe<sub>2</sub>O<sub>4</sub> spinel ferrite nanoparticles *J. Colloid. Interface. Sci.* **2013**, *398*, 152-160, DOI: 10.1016/j.jcis.2013.02.021.
- [47] Anbia, M.; Salehi, S., Removal of acid dyes from aqueous media by adsorption onto aminofunctionalized nanoporous silica SBA-3. *Dyes Pigm.* **2012**, *94*, 1-9, DOI: 10.1016/j.dyepig.2011.10.016.
- [48] Qin, Q.; Ma, J.; Liu, K., Adsorption of anionic dyes on ammonium-functionalized MCM-41. *J. Hazard. Mater.* **2009**, *162*, 133-139, DOI: 10.1016/j.jhazmat.2008.05.016.
- [49] Cheung, W. H.; Szeto, Y. S.; McKay, G., Intraparticle diffusion processes during acid dye adsorption onto chitosan. *Bioresour. Technol.* **2007**, *98*, 2897-2904, DOI: 10.1016/j.biortech.2006.09.045.
- [50] Gomez, V.; Larrechi, M.S.; Callao, M.P., Kinetic and adsorption study of acid dye removal using activated carbon. *Chemosphere* **2017**, *69*, 1151-1158, DOI: org/10.1016/j.chemosphere.2007.03.076.
- [51] Shirzad Siboni, M.; Jafari, S. J.; Giahi, O.; Kim, I.; Lee, S. M.; Yang, J. K., Removal of acid blue 113 and reactive black 5 dyes from aqueous solutions by activated red mud, *J. Ind. Eng. Chem.* **2014**, *20*, 1432-

- 1437, DOI: org/10.1016/j.jiec.2013.07.028.
- [52] Nekouei, F.; Nekouei, Sh.; Tyagi, I.; Kumar Gupta, V., Kinetic, thermodynamic and isotherm studies for Acid Blue 129 removal from liquids using copper oxide nanoparticle-modified activated carbon as a novel adsorbent, *J. Mol. Liq.* **2015**, *201*, 124-133, DOI: org/10.1016/j.molliq.2014.09.027.
- [53] Torabinejad, A.; Nasirizadeh, N.; Yazdanshenas, M. E.; Tayebi, H. A., Synthesis of conductive polymer-coated mesoporous MCM-41 for textile dye removal from aqueous media, *J. Nanostruct. Chem.* **2017**, *7*, 217-229, DOI: 10.1007/s40097-017-0232-7.
- [54] Kang, J. K.; Park, H. A.; Kim, J. H.; Lee, C. G.; Kim, S. B., Ammonium-functionalized mesoporous silica MCM-41 for phosphate removal from aqueous solutions, *Desalin. Water Treat.* **2015**, 1-13, DOI: org/10.1080/19443994.2015.1038590.
- [55] Arica, T. A.; Ayas, E.; Arica, M. Y., Magnetic MCM-41 silica particles grafted with poly (glycidylmethacrylate) brush: Modification and application for removal of direct dyes, *Microporous Mesoporous Mater.* **2017**, *243*, 164-175, DOI: 10.1016/j.micromeso.2017.02.011.
- [56] Binaeian, E.; Tayebi, H. A.; Shokui Rad, A.; Afrashteh, S., Adsorption of acid blue on synthesized polymeric nanocomposites, PPy/MCM-41 and PANi/MCM-41: Isotherm, thermodynamic and kinetic studies, *J. Macromol. Sci. A.* **2018**, *0*, 1-11, DOI: org/10.1080/10601325.2018.1424554.
- [57] Shabandokht, M.; Binaeian, E.; Tayebi, H. A., Adsorption of food dye Acid red 18 onto polyaniline-modified rice husk composite: isotherm and kinetic analysis, *Desalin. Water Treat.* **2016**, 1-13, DOI: 10.1080/19443994.2016.1172982.
- [58] Ghaedi, M., Comparison of cadmium hydroxide nanowires and silver nanoparticles loaded on activated carbon as new adsorbents for efficient removal of Sunset yellow: Kinetics and equilibrium study, *Spectrochim. Acta Part A: Mol. Biomol. Spectrosc.* **2012**, *94*, 346-351, DOI: 10.1016/j.saa.2012.02.097.
- [59] Torabinejad, A.; Nasirizadeh, N.; Yazdanshenas, M. E.; Tayebi, H. A., Synthesis of conductive polymer-coated mesoporous MCM-41 for textile dye removal from aqueous media. *J. Nanostruct. Chem.* **2017**, *7*, 217-229, DOI: 10.1007/s40097-017-0232-7.